A. Muzhikyan, A. M. Farid, and K. Youcef-Toumi, "An Enhanced Method for Determination of the Regulation Reserves," in IEEE American Control Conference, (Los Angeles, CA, USA), pp. 1–8, 2015.

An Enhanced Method for the Determination of the Regulation Reserves

Aramazd Muzhikyan[1], Amro M. Farid[2] and Kamal Youcef-Toumi[3]

***Abstract*—Generation reserves are the key resource for balancing power system generation and consumption. Reserves are used to mitigate any imbalances due to uncertainty and variability. However, as a costly commodity, the amount of reserves should be carefully assessed to maintain the cost of power system operations at its minimum. Currently, reserve requirement determination is based upon *a posteriori* methods that use the experience of power system operators and established assumptions. While these assumptions have been made out of a level of engineering practicality, they may not be formally true given the numerical evidence. The two prequels to this work presented methods for determination of the load following and ramping reserve requirements *a priori*. This paper now uses a similar methodology to determine the *regulation* reserve requirement.**

I. INTRODUCTION

Power balance is one of the key requirements for power system reliable operations. To achieve this, power system operators schedule the available generation units to meet the real-time demand. However, certain factors, such as forecast error and load variability, make matching the scheduled generation and the actual demand practically impossible. Moreover, similar factors work against power system balancing in the real-time operations. Normally, the impacts of forecast error and variability are compensated by scheduling additional generation capacity called reserves. This paper adopts the reserve classification as presented in [1], [2]. Three types of reserves operating in different timescales are distinguished in this paper, namely, load following, ramping and regulation reserves. While analytical methods for determination of load following and ramping reserve requirements have been reported in the literature [3], [4], the determination of the*appropriate* regulation reserve requirement is still an open research question.

Currently, the industrial practice and academic literature on reserves requirement determination follows a common theme. According to [5], the requirement of each type of reserve is determined *a posteriori* from the historical experience of power system operations. The data for forecast error or net load variability is used to determine the standard deviation of potential imbalances σ. Then, the quantities of each type of reserve are defined to cover the appropriate confidence interval in compliance with the North American Electric Reliability Corporation (NERC) or industrial balancing requirements. NERC defines the minimum score for the Control Performance Standard 2 (CPS2) equal to 90% [6], while the industry standard is 95% [7]. Normally, the load following reserve requirement is chosen 2σ or 3σ, while the regulation reserve requirement is 5σ or 6σ [5], [8]–[10].

The following assumptions are normally held in the industrial and academic literature when calculating regulation reserve requirement for the next relevant period of time:

Assumption 1. ***Invariant Probability Density Function of Imbalances:*** *The power system imbalances measured over the previous period will have the same probability distribution shape in the next period. Usually, a normal distribution is assumed.*

Assumption 2. ***Equivalence of Standard Deviations:*** *The standard deviation of power system imbalances is equivalently determined by either the net load variability or the forecast error. Some studies use the variability [5], [11], [12], while others use the forecast error [10], [13]–[15].*

Assumption 3. ***Invariant Standard Deviation of Imbalances:*** *The power system imbalances measured over the previous period will have the same standard deviation in the next period.*

Assumption 4. ***Non-dependence on Power System Operator Decisions & Control:*** *According to Assumption 2, the standard deviation of power system imbalances does not depend on the endogenous characteristics of the power system operator decisions and control, and only depends on net load variability and forecast error, which can be viewed as exogenous disturbances to the power system operation and control.*

While these assumptions have been made out of a level of engineering practicality, it is unlikely that they are formally true. Assumption 1 states that power system imbalances retain normal distribution from one period to the next, which has no numerical evidence [16]–[18]. Regarding Assumption 2, a perfectly forecasted but highly variable load may still require more regulation reserves than a modestly variable net load [19]. Therefore, the regulation reserve requirement is more likely to depend on both variability and forecast error. Also, while Assumption 3 suggests that power system does not evolve in a long term, variables, such as the variable energy resource (VER) penetration level and capacity factor, forecast

[1]Aramazd Muzhikyan is with the Department of Engineering Systems and Management, Masdar Institute of Science and Technology, PO Box 54224, Abu Dhabi, UAE amuzhikyan@masdar.ac.ae

[2]Amro M. Farid is with Faculty of Engineering Systems and Management, Masdar Institute of Science and Technology, PO Box 54224, Abu Dhabi, UAE afarid@masdar.ac.ae, and a Visiting Scientist at MIT Mechanical Engineering, 77 Massachusetts Avenue Cambridge, MA 02139, USA amfarid@mit.edu

[3]Kamal Youcef-Toumi is with Faculty of Mechanical Engineering, Massachusetts Institute of Technology, 77 Massachusetts Avenue Cambridge, MA 02139, USA youcef@mit.edu

error, net load variability, and real-time balancing time step, have the potential to change over time. The recent requirement of Federal Energy Regulatory Commission (FERC) to change the minimum frequency of the balancing market from 1 hour to 15 minutes is a good example. A more detailed discussion of the potential invalidity of these assumptions can be found in [19].

The two prequels to this work [3], [4] presented enhanced methods for determination of load following and ramping reserve requirements *a priori* with a set of assumptions that are more closely supported by numerical evidence and analytical models. This paper now uses a similar methodology to determine the requirement of *regulation* reserves. The paper is organized as follows. Section II provides the background of the problem and the fundamental definitions, Section III presents the methodology of the regulation reserve requirement calculation and Section IV summarizes the results and presents the future work.

II. BACKGROUND

This section introduces power system enterprise control and the fundamental definitions necessary for the regulation reserves calculation methodology presented in the following section.

A. Power Grid Enterprise Control

In this paper, the power system balancing operations are modeled as an enterprise control with three-layer, namely resource scheduling, balancing actions and regulation service, as presented in Fig. 1. Each consecutive stage operates at a smaller timescale, that allows successive improvements of power balance.

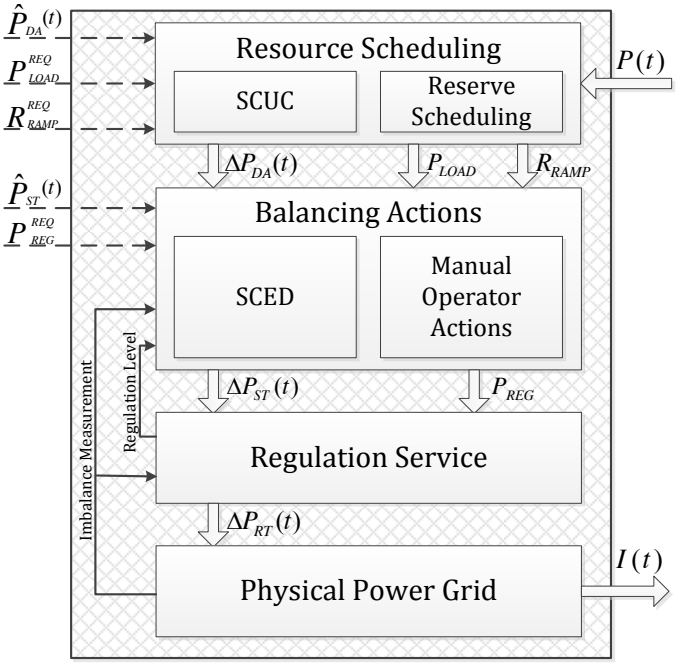

Figure 1: A three-layer power grid enterprise control model

At the first stage, the security-constrained unit commitment (SCUC) schedules the generation units based on the day-ahead net load forecast $\hat{P}_{DA}(t)$. Due to forecast inaccuracy, imbalances remain at the SCUC output as a difference between the real-time net load $P(t)$ and its forecast:

$$\Delta P_{DA}(t) = P(t) - \hat{P}_{DA}(t) \tag{1}$$

Power system operators also schedule load following reserves to mitigate the imbalance (1) in the next stage:

$$P_{res} = \beta_{DA}\,\sigma_{DA} \tag{2}$$

where σ_{DA} is the assumed standard deviation of (1) and β_{DA} is the confidence interval multiplier of σ_{DA}.

At the second stage, the real-time market implemented as a security-constrained economic dispatch (SCED) re-dispatches the generators based on the short-term net load forecast $\hat{P}_{ST}(t)$. Due to forecast inaccuracy, imbalances remain at the SCED output:

$$\Delta P_{ST}(t) = P(t) - \hat{P}_{ST}(t) \tag{3}$$

Imbalances at this stage are smaller since SCED uses a more accurate forecast and operates at a smaller timescale.

At the third stage, the regulation service operates to mitigates any residual imbalance. The regulation reserve requirement also can be presented similar to (2):

$$P_{reg} = \beta_{ST}\,\sigma_{ST} \tag{4}$$

where σ_{ST} is the assumed standard deviation of the input imbalance (3) and β_{ST} is the confidence interval multiplier. If appropriate amounts of each reserve are procured, the residual imbalance $I(t)$ stays within the acceptable range.

B. Fundamental Definitions

This section presents the definitions of fundamental concepts used in the regulation reserve requirement calculation methodology.

Definition 1. Penetration Level (π)*: The installed VER capacity P_V^{max} normalized by the system peak load P_L^{peak} [20]:*

$$\pi = P_V^{max}/P_L^{peak} \tag{5}$$

Definition 2. VER Capacity Factor (γ)*: The average VER power output $P_V(t)$ per installed capacity taken over a period T_0 (e.g. 1 year) [3]:*

$$\gamma = \frac{\overline{P^V(t)}}{P_V^{max}} \tag{6}$$

That T_0 is over the duration of a planning time scale allows the assumption that T_0 is large enough to allow the analysis of the given dataset with $T_0 \to \infty$.

Definition 3. Variability (A)*: Given the choice of the output $P(t)$ (e.g. the VER generation, the load, the net load), the variability is the root-mean-square of that output's rate normalized by the root-mean-square of that output [3], [4]:*

$$A = \frac{rms\,(\mathrm{d}P(t)/\mathrm{dt})}{rms(P(t))} \tag{7}$$

It is known from the literature that VER and load power spectra have distinctive shapes [21], [22]. Thus, the way to

manipulate the variability of the profile while keeping its spectral shape is temporal scaling of the profile. Assume that a base profile $P_0(t)$ has a variability A_0 and $P(t)$ is defined as:

$$P(t) = P_0(\alpha t) \tag{8}$$

According to (7):

$$A = \frac{rms\left(\mathrm{d}P_0(\alpha t)/\mathrm{dt}\right)}{rms(P_0(\alpha t))} = \alpha \cdot \frac{rms\left(\mathrm{d}P_0(\alpha t)/\mathrm{d}\left(\alpha \mathrm{t}\right)\right)}{rms(P_0(t))} = \alpha A_0 \tag{9}$$

Thus, α is the variability of the given profile normalized by the base variability A_0 [3]:

$$\alpha = \frac{A}{A_0} \tag{10}$$

Next, definitions regarding forecast error are introduced. The forecast error indicates the deviation between the actual and forecasted values and can be defined by various measures such as mean absolute error (MAE), mean square error (MSE) [23]. Often the load and VER forecast errors are normalized by the peak load and the installed capacity respectively.

Definition 4. Load Forecast Error (ε_L)*: The standard deviation of the difference between the actual and forecasted load normalized by the peak load [3]:*

$$\varepsilon_L = \frac{\sqrt{\frac{1}{n}\sum_{k=0}^{n}\left(P_k^L - \hat{P}_k^L\right)^2}}{P_L^{peak}} \tag{11}$$

Definition 5. VER Forecast Error (ε_V)*: The standard deviation of the difference between the actual and forecasted VER outputs normalized by the installed capacity [3]:*

$$\varepsilon_V = \frac{\sqrt{\frac{1}{n}\sum_{k=0}^{n}\left(P_k^V - \hat{P}_k^V\right)^2}}{P_V^{max}} \tag{12}$$

This work assumes that the forecast deviation of both load and VER have zero average:

$$\sum_{k=0}^{n}\left(P_k - \hat{P}_k\right) = \sum_{k=0}^{n}\left(P_k^L - \hat{P}_k^L\right) = \sum_{k=0}^{n}\left(P_k^V - \hat{P}_k^V\right) = 0 \tag{13}$$

Also, it is assumed that the forecast errors of load and VER are not correlated, i.e., for any integer m:

$$\sum_{k=0}^{n}\left(P_k^L - \hat{P}_k^L\right)\left(P_{k+m}^V - \hat{P}_{k+m}^V\right) = 0 \tag{14}$$

Finally, the definitions of the perfect and forecasted balancing profiles are introduced as presented in Fig. 2. In the real-time market, the generation units constantly adjust their outputs to meet the actual demand. The SCED problem determines the generator levels for the next time step based on the short-term net load forecast. In the case of a perfect forecast, the generation is expected to ramp linearly from its current level to the one step ahead value of the net load. However, the presence of the forecast error alters the actual generation profile.

Definition 6. Perfect Balancing Profile*: Given the choice of the output P(t) (e.g. the VER generation, the load, the net load), the perfect balancing profile is a piecewise linear function that connects the samples of P(t) with period T:*

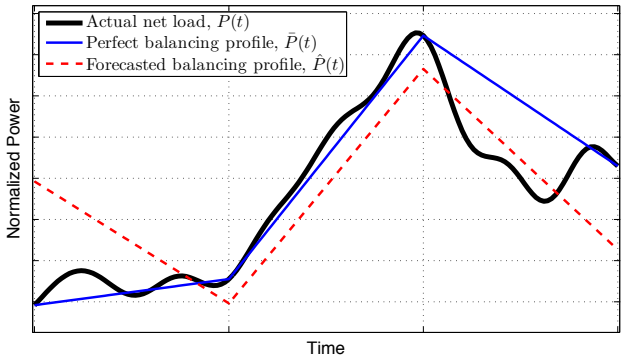

Figure 2: Actual net load, perfect and forecasted balancing profiles

$$\bar{P}(t) = P_k + \frac{P_{k+1} - P_k}{T} \cdot t, \quad kT \le t \le (k+1)T \tag{15}$$

Definition 7. Forecasted Balancing Profile*: Given the choice of the output P(t) (e.g. the VER generation, the load, the net load), the forecasted balancing profile is a piecewise linear function that connects the forecasts of P(t) with period T:*

$$\hat{P}(t) = \hat{P}_k + \frac{\hat{P}_{k+1} - \hat{P}_k}{T} \cdot t, \quad kT \le t \le (k+1)T \tag{16}$$

III. REGULATION RESERVE REQUIREMENT CALCULATION METHODOLOGY

As stated in the Section II, the real-time balancing market is implemented as a SCED problem. Due to the following factors the real-time market *never* matches the generation and actual net load:

- **Forecast error.** The SCED problem is solved based on the short-term net load forecast. Since each forecasting process has limited accuracy, the resulting forecast error contributes to the mismatch.
- **Balancing time step.** While the SCED problem has a limited time resolution, usually $5-15$ minutes, the actual net load changes constantly. This makes exact matching of the generation and net load impossible.

A. The Strategy

The current paper seeks to test Assumptions 1-4 and propose an analytical model that changes the regulation reserve requirement determination framework from assumptions to equations. As the first step, an analytical expression for the standard deviation of the potential imbalances is derived that contains the system parameters explicitly:

$$\sigma\left(\pi, \gamma, \alpha_L, \alpha_L, \varepsilon_L, \varepsilon_V, T\right) \tag{17}$$

This expression provides an *a priori* determination of how regulation reserve requirement changes as the system evolves and hence is sufficient to comprehensively test the validity of Assumptions 2-4. Next, the shape of the probability density function of the potential imbalances is studied under different scenarios to test the credibility of Assumption 1. Such an

analysis helps to numerically determine β_{ST} in (4) and gives the final estimate of the regulation reserve requirement.

This strategy gains further importance by virtue of the fact that the major part of the derivation of (17) is carried out in the spectral domain. Previous work in the literature has shown that the power spectra of VER generation and load have distinctive shapes [21], [22] which may be described by the very same parameters as in (17). Therefore, the method presented in this paper allows a regulation reserve requirement calculation which may be generalized to different VER integration scenarios.

B. The Standard Deviation of Imbalances

This section is devoted to the calculation of the standard deviation of imbalance.

1) The Standard Deviation: By definition, the standard deviation of imbalance (3) is:

$$\begin{aligned}
\sigma^2 &= \frac{1}{T_0}\int_0^{T_0}\Big(P(t)-\hat{P}(t)\Big)^2\mathrm{dt} = \\
&= \frac{1}{T_0}\int_0^{T_0}\Big(\big(P(t)-\bar{P}(t)\big)+\big(\bar{P}(t)-\hat{P}(t)\big)\Big)^2\mathrm{dt} = \\
&= \frac{1}{T_0}\int_0^{T_0}\Big(P(t)-\bar{P}(t)\Big)^2\mathrm{dt}+\frac{1}{T_0}\int_0^{T_0}\Big(\bar{P}(t)-\hat{P}(t)\Big)^2\mathrm{dt}+ \\
&+\frac{2}{T_0}\int_0^{T_0}\Big(P(t)-\bar{P}(t)\Big)\Big(\bar{P}(t)-\hat{P}(t)\Big)\mathrm{dt} = \sigma_1^2+\sigma_2^2+2\sigma_{12}^2
\end{aligned} \tag{18}$$

Each component is calculated separately. Using (15) and (16), σ_{12} is calculated as follows:

$$\begin{aligned}
\sigma_{12}^2 &= \frac{1}{T_0}\int_0^{T_0}\Big(P(t)-\bar{P}(t)\Big)\Big(\bar{P}(t)-\hat{P}(t)\Big)\mathrm{dt} = \\
&= \frac{1}{nT}\int_0^{nT}\Big(P(t)-\bar{P}(t)\Big)\Big(\bar{P}(t)-\hat{P}(t)\Big)\mathrm{dt} = \\
&= \frac{1}{n}\sum_{k=0}^{n-1}\left[\frac{1}{T}\int_{kT}^{(k+1)T}\Big(P(t)-\bar{P}(t)\Big)\times\right. \\
&\left.\times\left(\Big(P_k^L-\hat{P}_k^L\Big)+\frac{\big(P_{k+1}^L-\hat{P}_{k+1}^L\big)-\big(P_k^L-\hat{P}_k^L\big)}{T}\cdot t\right)\mathrm{dt}\right] = \\
&= \frac{1}{n}\sum_{k=0}^{n-1}\left[\Big(P_{k+1}^L-\hat{P}_{k+1}^L\Big)\frac{1}{T}\int_{kT}^{(k+1)T}\frac{t}{T}\cdot\Big(P(t)-\bar{P}(t)\Big)\mathrm{dt}\right]+ \\
&+\frac{1}{n}\sum_{k=0}^{n-1}\left[\Big(P_k^L-\hat{P}_k^L\Big)\frac{1}{T}\int_{kT}^{(k+1)T}\Big(1-\frac{t}{T}\Big)\cdot\Big(P(t)-\bar{P}(t)\Big)\mathrm{dt}\right]
\end{aligned} \tag{19}$$

where $n = T_0/T$ is the integer number of T intervals in the data set. The two terms of (19) are cross-covariances between the forecast error term and the integral difference of the actual and the perfect profiles. This term should be zero, since presence of any cross-covariance can be used to enhance the forecasting technique. This statement is also verified numerically.

Next, σ_2 is calculated as follows:

$$\begin{aligned}
\sigma_2^2 &= \frac{1}{T_0}\int_0^{T_0}\big(\bar{P}(t)-\hat{P}(t)\big)^2\mathrm{dt} = \\
&= \frac{1}{T_0}\int_0^{T_0}\Big(\big(\bar{P}^L(t)-\hat{P}^L(t)\big)-\big(\bar{P}^V(t)-\hat{P}^V(t)\big)\Big)^2\mathrm{dt} = \\
&= \frac{1}{T_0}\int_0^{T_0}\Big(\bar{P}^L(t)-\hat{P}^L(t)\Big)^2\mathrm{dt}+\frac{1}{T_0}\int_0^{T_0}\Big(\bar{P}^V(t)-\hat{P}^V(t)\Big)^2\mathrm{dt}- \\
&-\frac{2}{T_0}\int_0^{T_0}\Big(\bar{P}^L(t)-\hat{P}^L(t)\Big)\Big(\bar{P}^V(t)-\hat{P}^V(t)\Big)\mathrm{dt} = \\
&= \sigma_{2L}^2+\sigma_{2V}^2-2\sigma_{2LV}^2
\end{aligned} \tag{20}$$

Using (15) and (16), σ_{2L} can be written as follows:

$$\begin{aligned}
\sigma_{2L}^2 &= \frac{1}{T_0}\int_0^{T_0}\Big(\bar{P}^L(t)-\hat{P}^L(t)\Big)^2\mathrm{dt} = \frac{1}{nT}\int_0^{nT}\Big(\bar{P}^L(t)-\hat{P}^L(t)\Big)^2\mathrm{dt} = \\
&= \frac{1}{n}\sum_{k=0}^{n-1}\frac{1}{T}\int_{kT}^{(k+1)T}\Big(\bar{P}^L(t)-\hat{P}^L(t)\Big)^2\mathrm{dt} = \\
&= \frac{1}{n}\sum_{k=0}^{n-1}\frac{1}{T}\int_{kT}^{(k+1)T}\left[\Big(P_k^L-\hat{P}_k^L\Big)+\frac{\big(P_{k+1}^L-\hat{P}_{k+1}^L\big)-\big(P_k^L-\hat{P}_k^L\big)}{T}\cdot t\right]^2\mathrm{dt} = \\
&= \frac{1}{n}\sum_{k=0}^{n-1}\frac{1}{T}\int_{kT}^{(k+1)T}\left[\frac{\big(\big(P_{k+1}^L-\hat{P}_{k+1}^L\big)-\big(P_k^L-\hat{P}_k^L\big)\big)^2}{T^2}\cdot t^2+\right. \\
&\left.+\Big(P_k^L-\hat{P}_k^L\Big)^2+2\cdot\Big(P_k^L-\hat{P}_k^L\Big)\frac{\big(P_{k+1}^L-\hat{P}_{k+1}^L\big)-\big(P_k^L-\hat{P}_k^L\big)}{T}\cdot t\right]\mathrm{dt} = \\
&= \frac{1}{n}\sum_{k=0}^{n-1}\frac{\big(P_k^L-\hat{P}_k^L\big)^2+\big(P_{k+1}^L-\hat{P}_{k+1}^L\big)^2+\big(P_k^L-\hat{P}_k^L\big)\big(P_{k+1}^L-\hat{P}_{k+1}^L\big)}{3}
\end{aligned} \tag{21}$$

σ_{2V} and σ_{2LV} are calculated similarly. Since σ_{2LV} consists of cross terms between load and VER, according to (14) it is zero. The first two terms of σ_{2L} are the standard deviation and the third term is the single lag auto-covariance of the load forecast error. Thus, using the forecast error definitions (11) and (12), σ_{2L} and σ_{2V} can be written as:

$$\sigma_{2L} = \varepsilon_L\cdot\sqrt{\frac{2+\rho_L^2}{3}}\cdot P_L^{peak} \tag{22}$$

$$\sigma_{2V} = \varepsilon_V\cdot\sqrt{\frac{2+\rho_V^2}{3}}\cdot\pi\cdot P_L^{peak} \tag{23}$$

where ρ_L and ρ_V are auto-correlations of load and VER forecast errors respectively.

Normalized load and VER profiles are used for σ_1 calculation:

$$P^L(t) = \frac{P^L(t)}{P_L^{peak}}\cdot P_L^{peak} = p^L(t)\cdot P_L^{peak} \tag{24}$$

$$P^V(t) = \frac{P^V(t)}{\overline{P^V(t)}}\cdot\frac{\overline{P^V(t)}}{P_V^{max}}\cdot\frac{P_V^{max}}{P_L^{peak}}\cdot P_L^{peak} = p^V(t)\cdot\gamma\cdot\pi\cdot P_L^{peak} \tag{25}$$

The same normalizations are used for $\bar{P}^L(t)$ and $\bar{P}^V(t)$ correspondingly. Drawing upon (18), the expression for σ_1 with normalized profiles is the following:

$$\sigma_1^2 = \frac{1}{T_0}\int_0^{T_0}\left(P(t)-\bar{P}(t)\right)^2 \mathrm{dt} =$$
$$= \frac{1}{T_0}\int_0^{T_0}\left[\left(P^L(t)-\bar{P}^L(t)\right)-\left(P^V(t)-\bar{P}^V(t)\right)\right]^2 \mathrm{dt} =$$
$$= \frac{1}{T_0}\int_0^{T_0}\left(P^L(t)-\bar{P}^L(t)\right)^2 \mathrm{dt} + \frac{1}{T_0}\int_0^{T_0}\left(P^V(t)-\bar{P}^V(t)\right)^2 \mathrm{dt} -$$
$$- \frac{2}{T_0}\int_0^{T_0}\left[\left(P^L(t)-\bar{P}^L(t)\right)\left(P^V(t)-\bar{P}^V(t)\right)\right] \mathrm{dt} =$$
$$= \left(P_L^{peak}\right)^2 \frac{1}{T_0}\int_0^{T_0}\left(p^L(t)-\bar{p}^L(t)\right)^2 \mathrm{dt} +$$
$$+ \gamma^2\pi^2\cdot\left(P_L^{peak}\right)^2 \frac{1}{T_0}\int_0^{T_0}\left(p^V(t)-\bar{p}^V(t)\right)^2 \mathrm{dt} -$$
$$- 2\gamma\pi\left(P_L^{peak}\right)^2 \frac{1}{T_0}\int_0^{T_0}\left(p^L(t)-\bar{p}^L(t)\right)\left(p^V(t)-\bar{p}^V(t)\right) \mathrm{dt} =$$
$$= \left(\sigma_{1LL}^2+\gamma^2\pi^2\cdot\sigma_{1VV}^2-2\gamma\pi\cdot\sigma_{1LV}^2\right)\left(P_L^{peak}\right)^2 \tag{26}$$

The rest of this section is devoted to the calculations of σ_{1LL}, σ_{1VV} and σ_{1LV}. Since all three components have the same form, the calculations are performed for a general case:

$$\sigma_{1xy}^2 = \frac{1}{T}\int_0^{T}\left(p^x(t)-\bar{p}^x(t)\right)\left(p^y(t)-\bar{p}^y(t)\right)\mathrm{dt} \tag{27}$$

where x and y can refer to both load and VER. As mentioned in Section III-A, the calculations of (27) is performed in the spectral domain. According to the Parseval's theorem:

$$\sigma_{1xy}^2 = \int_{-\infty}^{+\infty} E\left[\left(P^x(\omega)-\bar{P}^x(\omega)\right)^*\left(P^y(\omega)-\bar{P}^y(\omega)\right)\right]\mathrm{d}\omega \tag{28}$$

The goal at this stage is to express $\bar{P}^x(\omega)$ and $\bar{P}^y(\omega)$ in terms of $P^x(\omega)$ and $P^y(\omega)$ respectively. Since only linear operations are used in the calculations, the variability can be incorporated into the following expressions [3]:

$$\bar{P}^x(\omega) = \bar{P}\left(\omega, \frac{1}{\sqrt{\alpha}}P^x\left(\frac{\omega}{\alpha}\right)\right) = \frac{1}{\sqrt{\alpha}}\bar{P}\left(\omega, P^x\left(\frac{\omega}{\alpha}\right)\right) \tag{29}$$
$$\bar{P}^y(\omega) = \bar{P}\left(\omega, \frac{1}{\sqrt{\alpha}}P^y\left(\frac{\omega}{\alpha}\right)\right) = \frac{1}{\sqrt{\alpha}}\bar{P}\left(\omega, P^y\left(\frac{\omega}{\alpha}\right)\right) \tag{30}$$

Substituting (29) and (30) into (28) leads to:

$$\sigma_{1xy}^2 = \int_{-\infty}^{+\infty} E\left[\left(P^x\left(\frac{\omega}{\alpha}\right)-\bar{P}\left(\omega, P^x\left(\frac{\omega}{\alpha}\right)\right)\right)^*\times\right.$$
$$\left.\times\left(P^y\left(\frac{\omega}{\alpha}\right)-\bar{P}\left(\omega, P^y\left(\frac{\omega}{\alpha}\right)\right)\right)\right]\mathrm{d}\left(\frac{\omega}{\alpha}\right) \tag{31}$$

Since the integration in (31) goes over $(-\infty;+\infty)$, the substitution $\omega/\alpha=\omega$ can be made:

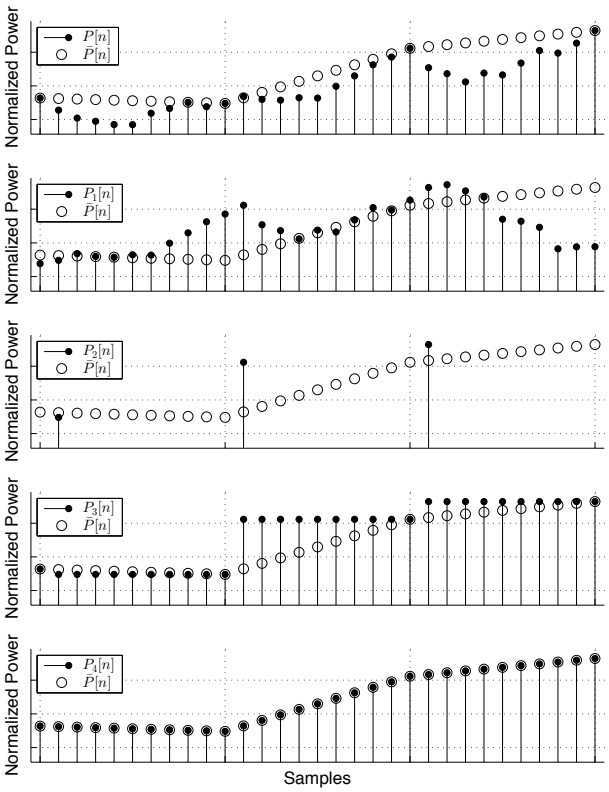

Figure 3: Four steps of signal processing

$$\sigma_{1xy}^2 = \int_{-\infty}^{+\infty} E\left[\left(P^x(\omega)-\bar{P}\left(\alpha\omega, P^x(\omega)\right)\right)^*\times\right.$$
$$\left.\times\left(P^y(\omega)-\bar{P}\left(\alpha\omega, P^y(\omega)\right)\right)\right]\mathrm{d}\omega \tag{32}$$

$\bar{P}^x(\omega)$ and $\bar{P}^y(\omega)$ are calculated similarly. Thus, only one is considered and the superscripts x, y are omitted. The following section is devoted to the time-domain demonstration of the processing steps, which clarifies the logic of the spectral domain operations later.

2) Time Domain Demonstration: Fig. 3 shows the four-step transformation from $p[n]$ into $\bar{p}[n]$:

Step 1: Phase Adjustment. To construct the perfect balancing profile (15), the last samples of each T interval need to be captured by downsampling. Since the downsampling starts from the first sample, the original profile should be shifted left by $N-1$ samples:

$$p_1[n] = p[n-(N-1)] \tag{33}$$

where $N = T/T_s$ is the number of samples in T. T_s is the data sampling period.

Step 2: Downsampling. Next, the profile is downsampled with period T:

$$p_2[n] = \begin{cases} p_1[n], & n = k\cdot N; \\ 0, & \text{otherwise.} \end{cases} \tag{34}$$

Step 3: Summing. This step turns single samples into rectangles for each interval. Since each interval contains only one

non-zero sample, summing over N samples yields the value of the non-zero sample for the whole interval:

$$p_3[n] = \sum_{k=0}^{N-1} p_2[n-k] \tag{35}$$

Step 4: Averaging. Averaging calculates the sliding window average of the input for one time step T to create linear ramps:

$$\bar{p}[n] = p_4[n] = \frac{1}{N}\sum_{k=0}^{N-1} p_3[n-k] \tag{36}$$

The next paragraph implements these four steps in the spectral domain.

3) Frequency Domain Calculations: The same processing steps described in the previous section are implemented in the spectral domain.

Step 1: Phase Adjustment. Using the translation property of the Fourier transform, (33) takes the following form in the spectral domain:

$$P_1(\omega) = P\left(\frac{\omega}{\alpha}\right)\cdot e^{j\omega(N-1)T_s} = P\left(\frac{\omega}{\alpha}\right)\cdot e^{j\omega(T-T_s)} \tag{37}$$

Step 2: Downsampling. The spectrum of the downsampled profile has the following form:

$$\begin{aligned} P_2(\omega) &= \frac{1}{N}\sum_{n=0}^{N-1} P_1\left(\omega - \frac{2\pi n}{T}\right) = \\ &= \frac{1}{N}\sum_{n=0}^{N-1}\left[P\left(\frac{1}{\alpha}\left(\omega - \frac{2\pi n}{T}\right)\right)e^{j\left(\omega-\frac{2\pi n}{T}\right)(T-T_s)}\right] = \\ &= \frac{1}{N}\sum_{n=0}^{N-1}\left[P\left(\frac{1}{\alpha}\left(\omega - \frac{2\pi n}{T}\right)\right)e^{j(\omega T-2\pi n)}e^{j\left(\omega-\frac{2\pi n}{T}\right)T_s}\right] = \\ &= \frac{1}{N}\sum_{n=0}^{N-1}\left[P\left(\frac{1}{\alpha}\left(\omega - \frac{2\pi n}{T}\right)\right)e^{-j\left(\omega-\frac{2\pi n}{T}\right)T_s}\right]e^{j\omega T} \end{aligned} \tag{38}$$

where $\exp(j2\pi n) = 1$ is used.

Step 3: Summing. Using the linearity and translation properties of the Fourier transform and the formula for the sum of geometric progression, (35) takes the following form in the spectral domain:

$$\begin{aligned} P_3(\omega) &= \sum_{n=0}^{N-1} P_2(\omega)e^{-j\omega nT_s} = P_2(\omega)\cdot\frac{1-e^{-j\omega NT_s}}{1-e^{-j\omega T_s}} = \\ &= \frac{1}{N}\sum_{n=0}^{N-1}\left[P\left(\frac{1}{\alpha}\left(\omega - \frac{2\pi n}{T}\right)\right)e^{-j\left(\omega-\frac{2\pi n}{T}\right)T_s}\right]\frac{1-e^{-j\omega T}}{1-e^{-j\omega T_s}}e^{j\omega T} \end{aligned} \tag{39}$$

Step 4: Averaging. Similar to the previous step, in the spectral domain (36) takes the following form:

$$\begin{aligned} \bar{P}(\omega) = P_4(\omega) &= \frac{1}{N}P_3(\omega)\frac{1-e^{-j\omega T}}{1-e^{-j\omega T_s}} = \\ &= \frac{1}{N^2}\sum_{n=0}^{N-1}\left[P\left(\frac{1}{\alpha}\left(\omega - \frac{2\pi n}{T}\right)\right)e^{-j\left(\omega-\frac{2\pi n}{T}\right)T_s}\right]\frac{\left(1-e^{-j\omega T}\right)^2}{\left(1-e^{-j\omega T_s}\right)^2}e^{j\omega T} \end{aligned} \tag{40}$$

4) Simplifications: Since accurate calculations require a sampling rate that is small enough to capture slightest variations of the data, it can be assumed that for proper calculations the data sampling rate should be much higher than its variability. Since the variability is also related to the spectral width of the data [3], this assumption implies that the spectral width of the data is much smaller than the sampling rate. As a result, the spectrum has negligible values at $\omega \gtrsim 1/T_s$. Thus, the following approximation is made using the Taylor series:

$$e^{-j\omega T_s} \approx 1 \tag{41}$$

The same applies to all shifted spectral copies and (40) can be rewritten as:

$$\bar{P}(\omega) = \frac{1}{N^2}\sum_{n=0}^{N-1}\left[P\left(\frac{1}{\alpha}\left(\omega - \frac{2\pi n}{T}\right)\right)\right]\frac{\left(1-e^{-j\omega T}\right)^2}{\left(1-e^{-j\omega T_s}\right)^2}e^{j\omega T} \tag{42}$$

Also, the multiplier $1/\left(1-e^{-j\omega T_s}\right)$ in (42) is a periodic function that resembles $1/\omega$ at low frequencies. Its multiplication by the sum of the shifted spectral copies makes the copies far from the center appear very small. Thus, it can be replaced by $1/\omega$. Moreover, since $1/\omega$ decays monotonically, it mitigates all the copies outside the range and, hence, the summation can be done over infinity. This also makes the final expression independent of the sampling frequency:

$$\bar{P}(\omega) = -\frac{1}{T^2}\sum_{n=0}^{N-1}\left[P\left(\frac{1}{\alpha}\left(\omega - \frac{2\pi n}{T}\right)\right)\right]\frac{\left(1-e^{-j\omega T}\right)^2}{\omega^2}e^{j\omega T} \tag{43}$$

Finally, making the substitution $\omega/\alpha \equiv \omega$ discussed in (31) and (32) leads to the final expression:

$$\bar{P}(\omega) = -\frac{1}{(\alpha T)^2}\sum_{n=0}^{N-1}\left[P\left(\omega - \frac{2\pi n}{\alpha T}\right)\right]\frac{\left(1-e^{-j\omega\alpha T}\right)^2}{\omega^2}e^{j\omega\alpha T} \tag{44}$$

According to (44), the variability and the real-time market step appear everywhere as multipliers. This means that the impact of increased variability on the regulation requirement can be effectively mitigated by reducing the real-time market step. Substituting (44) into (32), the regulation reserve requirement depends on the following components:

$$\rho\left(\omega - \frac{2\pi n}{\alpha T}, \omega - \frac{2\pi m}{\alpha T}\right) = E\left[P^*\left(\omega - \frac{2\pi n}{\alpha T}\right)P\left(\omega - \frac{2\pi m}{\alpha T}\right)\right] \tag{45}$$

for all values of m and n, which are the samples of the spectrum correlation function. The correlation happens between mixed copies of VER and load spectrum.

C. The Probability Distribution Shape Consideration

Once the standard deviation of imbalances has been calculated according to (17), the paper returns to the determination of β_{ST} found in (4). To that end, the probability distribution of (3) is studied, which also allows revising Assumption 1. The probability density function of imbalances is measured for different values of penetration level, forecast error and variability. Changing the capacity factor and the real-time market step would have similar impact as the penetration level and the variability respectively. Fig. 4 depicts the obtained probability density functions normalized to a unit standard deviation. The apparent large differences of the probability density profiles invalidate Assumption (1).

However, what is more important for the regulation reserve requirement calculation is confidence intervals for the given probabilities. Therefore, the associated family of cumulative

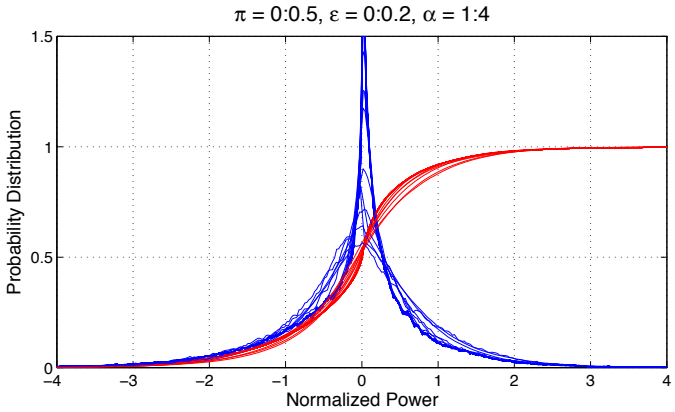

Figure 4: Probability density and cumulative probability functions for different values of π, ε and α

distribution functions is also drawn in Fig. 4. Although there is still a visible difference between them, only the 90% and 95% confidence intervals are interesting for the reserve requirement calculation. As Table I shows, 90% and 95% confidence intervals generally agree for the wide ranges of penetration levels, forecast errors and variabilities. The inaccuracy is defined here as the ratio of the standard deviation and average value. Thus, it can be concluded that the regulation reserve requirements for these two confidence intervals are:

$$P^{res}_{90\%} \approx 1.9\sigma \tag{46}$$

$$P^{res}_{95\%} \approx 2.4\sigma \tag{47}$$

where σ is calculated according to (18).

Table I: 90% and 95% confidence intervals

Percentage	Min	Max	Inaccuracy
5%	-1.8998	-1.5761	0.032
95%	1.3142	1.5495	0.033
2.5%	-2.4324	-1.9922	0.036
97.5%	1.7565	1.9624	0.020

IV. CONCLUSIONS AND FUTURE WORK

The framework, established in this works allows an assessment of power system regulation reserve requirements. It is based on analytical derivations of the standard deviation that shows that the reserve requirements depends on non-dimensional parameters of the power system and the net load. This results are contrary to the assumptions in the existing literature. As future research, a set of simulations will be performed to validate the proposed method more profoundly.

REFERENCES

[1] H. Holttinen, M. Milligan, E. Ela, N. Menemenlis, J. Dobschinski, B. Rawn, R. J. Bessa, D. Flynn, E. Gomez-Lazaro, and N. K. Detlefsen, "Methodologies to Determine Operating Reserves Due to Increased Wind Power," *Sustainable Energy, IEEE Transactions on*, vol. 3, no. 4, pp. 713–723, 2012.

[2] E. Ela, B. Kirby, E. Lannoye, M. Milligan, D. Flynn, B. Zavadil, and M. O'Malley, "Evolution of operating reserve determination in wind power integration studies," in *Power and Energy Society General Meeting, 2010 IEEE*, 2010, pp. 1–8.

[3] A. Muzhikyan, A. M. Farid, and K. Youcef-Toumi, "An Enhanced Method for the Determination of Load Following Reserves," in *American Control Conference 2014 (ACC2014)*, Portland, OR, 2014, pp. 926–933.

[4] ——, "An Enhanced Method for Determination of the Ramping Reserves," in *Under review: American Control Conference 2015 (ACC2015)*, Chicago, Ill., 2014, pp. 1–8.

[5] H. Holttinen, M. Milligan, B. Kirby, T. Acker, V. Neimane, and T. Molinski, "Using Standard Deviation as a Measure of Increased Operational Reserve Requirement for Wind Power," *Wind Engineering*, vol. 32, no. 4, pp. 355–377, 2008.

[6] North American Electric Reliability Corporation, "Reliability Standards for the Bulk Electric Systems of North America," *NERC Reliability Standards Complete Set*, pp. 1–10, 2012.

[7] D. A. Halamay, T. K. A. Brekken, A. Simmons, and S. McArthur, "Reserve Requirement Impacts of Large-Scale Integration of Wind, Solar, and Ocean Wave Power Generation," *Sustainable Energy, IEEE Transactions on*, vol. 2, no. 3, pp. 321–328, 2011.

[8] A. Robitaille, I. Kamwa, A. Oussedik, M. de Montigny, N. Menemenlis, M. Huneault, A. Forcione, R. Mailhot, J. Bourret, and L. Bernier, "Preliminary Impacts of Wind Power Integration in the Hydro-Quebec System," *Wind Engineering*, vol. 36, no. 1, pp. 35–52, Feb. 2012.

[9] T. Aigner, S. Jaehnert, G. L. Doorman, and T. Gjengedal, "The Effect of Large-Scale Wind Power on System Balancing in Northern Europe," *Sustainable Energy, IEEE Transactions on*, vol. 3, no. 4, pp. 751–759, 2012.

[10] B. C. Ummels, M. Gibescu, E. Pelgrum, W. L. Kling, and A. J. Brand, "Impacts of Wind Power on Thermal Generation Unit Commitment and Dispatch," *Energy Conversion, IEEE Transactions on*, vol. 22, no. 1, pp. 44–51, 2007.

[11] P. J. Luickx, E. D. Delarue, and W. D. D'haeseleer, "Effect of the generation mix on wind power introduction," *Renewable Power Generation, IET*, vol. 3, no. 3, pp. 267–278, 2009.

[12] C. W. Hansen and A. D. Papalexopoulos, "Operational Impact and Cost Analysis of Increasing Wind Generation in the Island of Crete," *Systems Journal, IEEE*, vol. 6, no. 2, pp. 287–295, 2012.

[13] Y. V. Makarov, P. V. Etingov, and J. Ma, "Incorporating Uncertainty of Wind Power Generation Forecast Into Power System Operation , Dispatch , and Unit Commitment Procedures," *Sustainable Energy, IEEE Transactions on*, vol. 2, no. 4, pp. 433–442, 2011.

[14] Y. V. Makarov, S. Lu, N. Samaan, Z. Huang, K. Subbarao, P. V. Etingov, J. Ma, R. P. Hafen, R. Diao, and N. Lu, "Integration of Uncertainty Information into Power System Operations," in *Power and Energy Society General Meeting, 2011 IEEE*, 2011, pp. 1–13.

[15] Y. V. Makarov, C. Loutan, J. Ma, and P. de Mello, "Operational Impacts of Wind Generation on California Power Systems," *Power Systems, IEEE Transactions on*, vol. 24, no. 2, pp. 1039–1050, 2009.

[16] B.-M. Hodge, D. Lew, M. Milligan, H. Holttinen, S. Sillanpää, E. Gómez-Lázaro, R. Scharff, L. Söder, X. G. Larsén, G. Giebel, D. Flynn, and J. Dobschinski, "Wind Power Forecasting Error Distributions: An International Comparison," National Renewable Energy Laboratory, Tech. Rep., 2012.

[17] B. Hodge and M. Milligan, "Wind Power Forecasting Error Distributions over Multiple Timescales," in *Power and Energy Society General Meeting, 2011 IEEE*. National Renewable Energy Laboratory, 2011, pp. 1–8.

[18] G. Giebel, R. Brownsword, G. Kariniotakis, M. Denhard, and C. Draxl, "The State-Of-The-Art in Short-Term Prediction of Wind Power: A Literature Overview," ANEMOS.plus, Tech. Rep., 2011.

[19] A. M. Farid and A. Muzhikyan, "The Need for Holistic Assessment Methods for the Future Electricity Grid," in *GCC Power 2013 Conference & Exhibition*, Abu Dhabi, UAE, 2013, pp. 1–13.

[20] C. Wang, Z. Lu, and Y. Qiao, "A Consideration of the Wind Power Benefits in Day-Ahead Scheduling of Wind-Coal Intensive Power Systems," *Power Systems, IEEE Transactions on*, vol. 28, no. 99, p. 1, 2012.

[21] J. Apt, "The spectrum of power from wind turbines," *Journal of Power Sources*, vol. 169, no. 2, pp. 369–374, June 2007.

[22] A. E. Curtright and J. Apt, "The character of power output from utility-scale photovoltaic systems," *Progress in Photovoltaics: Research and Applications*, vol. 16, no. 3, pp. 241–247, May 2008.

[23] C. Monteiro, R. Bessa, V. Miranda, A. Botterud, J. Wang, and G. Conzelmann, "Wind Power Forecasting: State-of-the-Art 2009," Argonne National Laboratory, Illinois, Tech. Rep., 2009.